Original Research (2026) 3(2); 45 - 60
https://doi.org/10.22103/VCBR.2026.25956.1098

Shahid Bahonar University of Kerman

Veterinary and Comparative Biomedical Research

ORIGINAL ARTICLE

Comparison of Varied Microfluidic Ratchet Designs on Sperm Sorting and Quality in Low-Quality Samples

Saeed Derakhshan [1], Ataallah Kamyabi [1*], Sareh Ashourzadeh [2], Tooraj Reza Mirshekari [2]

[1] *Department of Chemical Engineering, Faculty of Engineering, Shahid Bahonar University of Kerman, Kerman, Iran*
[2] *Afzalipour Clinical Center for Infertility, Afzalipour Hospital, Kerman University of Medical Sciences, Kerman, Iran*

Online ISSN: 3060-7663 **https://doi.org/10.22103/VCBR.2026.25956.1098**

***Correspondence**

Author's Email:
kamyabi@uk.ac.ir

Article History

Received: *23 September 2025*
Revised: *1 December 2025*
Accepted: *30 April 2026*
Published: *14 May 2026*

Keywords

Assisted Reproductive Techniques
Microchannel
Ratchet Microchannel
Sperm Separation

Abstract

Infertility affects approximately 17% of adults worldwide, with male factors contributing to 20–40% of cases. Conventional sperm selection methods, such as density gradient centrifugation and swim-up, can cause DNA damage via reactive oxygen species and mechanical stress, limiting their use in assisted reproductive technologies (ART), including intracytoplasmic sperm injection. Microfluidic systems provide a gentler alternative by exploiting sperm motility and morphology. Using polymethyl methacrylate sheets laser-engraved to create asymmetric ratchet geometries, four designs were evaluated at flow rates of 0.034 mL/min and 0.017 mL/min. Semen samples from patients with low sperm quality were injected, and output fractions were assessed for concentration, motility, morphology, and the sperm retrieval index (SRI), a composite metric normalized to World Health Organization standards. The results showed consistent improvements, with optimal designs yielding up to a fourfold increase in sperm concentration (e.g., from 10 to 40 million/mL) and over 20-fold SRI enhancement, particularly at the lower flow rate, which minimized shear stress and promoted rheotactic trapping of motile sperm. These findings suggest that ratchet microchannels offer a simple and effective approach for sperm enrichment and improving ART outcomes without the need for centrifugation.

How to cite this article: Saeed Derakhshan, Ataallah Kamyabi, Sareh Ashourzadeh, Tooraj Reza Mirshekari. Comparison of Varied Microfluidic Ratchet Designs on Sperm Sorting and Quality in Low-Quality Samples. *Veterinary and Comparative Biomedical Research*, 2026 3(2): 45 – 60. https://doi.org/10.22103/VCBR.2026.25956.1098

Introduction

Infertility represents a major global health concern, affecting nearly 17% of the adult population, approximately one in every six individuals, and imposing profound psychological, social, and economic burdens on couples (1). Male factors alone contribute to roughly 20% of infertility cases and serve as a cofactor in an additional 30–40% of cases (2). In assisted reproductive technologies (ART), especially intracytoplasmic sperm injection (ICSI), selecting spermatozoa with high motility, normal morphology, and intact DNA is fundamental to achieving optimal fertilization outcomes. Traditionally, sperm preparation and selection rely on density gradient centrifugation (DGC), direct swim-up, and wash-based techniques. Although these methods aim to enrich functional sperm and remove dead cells, leukocytes, and cellular debris, each approach carries limitations that restrict its efficiency and safety (3-6).

DGC, although effective in separating sperm populations based on density, exposes spermatozoa to substantial mechanical forces that generate reactive oxygen species (ROS) and increase the risk of DNA fragmentation. Such DNA damage can compromise embryo development and ART success. Additionally, DGC is relatively time-consuming and may retain spermatozoa with abnormal morphology. The swim-up technique, in contrast, relies on the sperm's intrinsic ability to migrate into fresh medium. Although this method is gentler and associated with lower ROS production, it typically yields limited sperm numbers, which is problematic in samples with severe oligospermia. Moreover, swim-up does not consistently eliminate sperm exhibiting DNA abnormalities. Overall, conventional centrifugation-based approaches lack scalability, require specialized equipment, and may negatively affect sperm morphology, thereby limiting their reliability in clinical practice (7-9). While assays such as TUNEL or SCSA can directly assess DNA integrity, they are technically demanding, expensive, and may compromise sperm viability, making them unsuitable as routine selection tools (10). Alternative approaches, including zeta potential–based selection and microfluidic techniques, have emerged to isolate high-quality sperm with minimal stress; however, these methods still require extensive clinical validation (11).

Microfluidics has become a powerful tool for manipulating fluids at the micrometer scale with exceptional precision, enabling fine control over flow fields and particle trajectories (12). In the context of sperm selection, microfluidic systems exploit inherent sperm characteristics, including motility, size, and morphology, to facilitate the isolation of functional sperm from heterogeneous semen samples (13). These platforms incorporate networks of microchannels and microstructures that leverage laminar flow, hydrodynamic gradients, or physical constraints to guide motile and morphologically normal sperm toward collection zones while excluding immotile or defective cells (14). Chemotaxis- and rheotaxis-based systems rely on sperm behavior under mild flow conditions or in response to chemical cues, thereby mimicking physiological transport in the female reproductive tract (15, 16). Other devices use microfilters or constrictions to differentiate sperm based on size or motility capacity (16).

Recent advances highlight the promise of microfluidics for improving sperm selection. Heidarnejad et al. (2024) developed a rheotaxis-based device that yielded sperm with enhanced motility, morphology, and viability compared with DGC (17). Phiphattanaphiphop et al. (2020) used COMSOL simulations and design of experiments to optimize bovine sperm sorting, achieving 96% efficiency with a strong correlation between computational and experimental results (18). Asghar et al. (2014) introduced a two-chamber system separated by a microporous membrane, improving motility and DNA integrity, with 8 µm pores performing best (19). Chinnasamy et al. (2018) created a biomimetic columnar array that isolated highly motile sperm in under 10 minutes, significantly improving motility, morphology, and DNA quality (20). Huang et al. (2014) integrated laminar flow with flow cytometry for the efficient separation of human sperm, achieving >92–95% survival (21). Wu et al. (2017) developed the FUSS device, which mimics natural sperm selection and enables high-throughput sorting (~200,000 sperm/min) with approximately 90% motile output (22). Collectively, these studies illustrate that microfluidic approaches can improve sperm quality while reducing mechanical and oxidative stress.

Microfluidic ratchet systems represent a particularly intriguing class of sorting devices. Ratchet effects arise when particles traverse asymmetric surfaces under external forcing or periodic modulation, generating directional transport. Active ratchets extend this concept to self-propelled particles, such as bacteria or sperm, allowing directional migration without external forces (23). Hulme et al. (2008) demonstrated that asymmetric microchannels could sort *E. coli* based on cell length by leveraging hydrodynamic interactions and turning behavior (24). Guidobaldi et al. (2014) showed that human sperm exhibit characteristic boundary-following behavior in microfluidic confinement, influenced by angled walls and asymmetric barriers (25). Coppola and Kantsler (2021) evaluated eight ratchet geometries for bacterial transport, showing that

curved ratchets minimize reorientation and trapping, thereby enhancing rectification efficiency (26). These findings underscore the relevance of asymmetric and funnel-like microstructures for guiding motile cells.

Huang et al. (2014) categorized microfluidic sperm-sorting technologies into passive, active, and externally driven systems, emphasizing the role of physiological guidance cues—rheotaxis, chemotaxis, and thermotaxis—in improving sperm selection (21). Structured microenvironments can reduce mechanical stress and ROS production, enhancing sperm function (27). Karimi et al. (2025) demonstrated that obstacle geometry modulates sperm navigation under flow, with conical features promoting upstream alignment and collective organization mechanisms that are beneficial for selective sperm transport (28). Bouloorchi et al. (2024) reviewed microfluidic ART technologies, highlighting commercial platforms such as ZyMōt that improve motility, DNA integrity, and pregnancy outcomes (29). Denissenko et al. (2012) showed that sperm follow predictable geometric trajectories influenced by boundary conditions, principles that are directly applicable to the design of ratchet structures for efficient sorting (30). More recent findings indicate that ratchet-based microfluidic devices can enhance sperm separation efficiency by 50–60% while reducing DNA damage (17, 31), and simplified microchannels have shown improvements in raw semen processing (17).

Although ratchet-based microfluidics shows promise, there is insufficient systematic analysis of how ratchet geometry, including asymmetry, curvature, density, and length, impacts sorting performance, particularly in low-quality semen samples characterized by poor motility, abnormal morphology, and low concentration. To address this gap, the present study designed and fabricated multiple ratchet configurations within polymethyl methacrylate (PMMA) microchannels using CO_2 laser engraving. The objective was to evaluate the effects of geometric variations on sperm recovery and quality. Key sperm parameters, including progressive motility, total motility, normal morphology, and concentration, were quantified using the SRI, a composite metric normalized to World Health Organization reference thresholds. Using controlled flow rates of 0.034 and 0.017 mL/min, raw semen samples from patients with oligoasthenospermia were tested to identify the geometric features that most effectively enhance sperm quality. Ultimately, this study aims to provide a foundation for integrating optimized ratchet-based microfluidic platforms into clinical ART workflows to improve fertilization outcomes and reduce dependence on centrifugation-based methods.

In the Theoretical Background section, Human sperm consists of a disc-shaped head with an elliptical cross-section and a flagellum, which serves as the primary locomotor organ (32). The flagellum is divided into a rigid midpiece and a flexible tail and is driven by the axoneme, a cylindrical structure typically 1–50 μm in length and 250 nm to 1 μm in radius (33).

The axoneme exhibits a characteristic “9+2” microtubule arrangement, in which a central pair of microtubules is surrounded by nine outer doublets, interconnected by nexin links for structural integrity (see Figure 2–4 for a cross-sectional view) (34). Flagellar bending is powered by dynein motor proteins, which hydrolyze ATP to induce sliding between adjacent microtubules, generating wave-like motions (35). In human sperm, these motions manifest as three-dimensional helical patterns, with the sperm rotating around its longitudinal axis [35]. Sperm navigation is not solely dependent on internal structure but is also profoundly influenced by external environmental factors. Several guidance mechanisms direct sperm toward the oocyte:

Chemotaxis: Human sperm respond to chemical gradients, such as progesterone, by altering flagellar beat patterns. This is mediated by calcium influx induced by progesterone, which modulates ion channels and hyperactivates motility (36).

Thermotaxis: Sperm exhibit sensitivity to temperature gradients, preferentially swimming toward warmer regions, which mimics the thermal environment of the female reproductive tract (37).

Rheotaxis: Fluid flows within the reproductive tract guide sperm orientation, enabling upstream swimming against gentle currents (38).

Passive Guidance Along Surfaces: Sperm tend to accumulate near boundaries due to hydrodynamic and steric interactions, a behavior observed in human, mouse, and bovine sperm (39). This surface-following navigation aids in traversing complex geometries within the female tract. Collectively, these mechanisms ensure efficient sperm migration, with theoretical models emphasizing the interplay between intrinsic propulsion and extrinsic cues for optimal fertilization success.

When approaching a solid wall, sperm, as microswimmers propelled by flagellar beating, generate a flow field resembling a force dipole. This flow induces hydrodynamic attraction toward the surface, causing sperm to maintain proximity and slide along the wall (28). Upon nearing the boundary, the flagellar waveform transitions from three-dimensional to two-dimensional, facilitating sustained propulsion without detachment. This zone ensures the head and tail nodes receive repulsive forces, preserving

a buffer distance that allows continued flagellar beating. Elgeti and Gompper (40) further explain that microswimmers near surfaces experience hydrodynamic entrapment due to interactions between their flow fields and the boundary, leading to "wall accumulation." This phenomenon is crucial for designing microfluidic channels, as it enhances sperm retention and sorting efficiency while minimizing oxidative stress.

In angled geometries, such as convex V-shaped vertices, sperm behavior shifts markedly. For sharp angles with curvature radii below 8 µm, sperm become trapped, a phenomenon termed "entrapment," due to spatial constraints preventing maneuvers (required space ≈ twice head radius + oscillation amplitude) (25). Numerical simulations reveal elevated densities at corners, with central areas depleted. As the vertex curvature radius exceeds 8 µm, a "trapping-to-escape transition" occurs, providing sufficient space for oscillation and rotation, facilitating detachment. Higher sperm density exacerbates collective trapping, while longer V-arm lengths increase entry rates without affecting escape, intensifying entrapment. To mitigate trapping, alternative designs incorporate U-shaped or curved barriers with larger curvatures, allowing maneuverability and directional guidance. In arrays of U- and ∩-shaped obstacles, sperm accumulate in intermediate regions without corner clustering. Slits with widths of approximately 15 µm enable controlled migration, creating a "geometric ratchet" effect in which flow in the "easy" direction exceeds that in the 'hard' direction due to asymmetric passage probabilities (24, 26). These theoretical insights, grounded in hydrodynamic models and empirical observations, inform microfluidic device design for sperm sorting, leveraging boundary interactions to enhance selectivity and viability in assisted reproductive technologies.

Materials and Methods

Experimental section

Polymethyl methacrylate (PMMA) sheets with a thickness of 2 mm were used as the base material for microchannel fabrication. The sperm culture medium consisted of HEPES-buffered human tubal fluid (HTF) supplemented with 10% human serum albumin (HSA). Raw semen samples were collected from patients diagnosed with low-quality sperm samples. All samples were obtained following written informed consent and in accordance with the ethical protocols approved by Shahid Bahonar University of Kerman (Ethics Code: IR.UK.REC.1401.009).

Ratchet microchannels were designed and fabricated on PMMA sheets using laser engraving. Several designs were prepared by varying key geometric parameters. Sealing of PMMA layers is commonly performed by thermal (fusion) bonding, in which the parts are pressed near or above PMMA's glass transition temperature (Tg ≈105–110 °C). Our process (120 °C at 2 bar for 90 min) falls within the ranges reported in the literature: studies typically heat-bonded PMMA at approximately 95–160 °C under a few bars of pressure for minutes to hours. For example, one study reports combining an ethanol pre-soak with UV exposure, followed by thermal pressing at 120 °C for 2 h under applied weight. Heating above Tg promotes polymer-chain interdiffusion and strong fusion bonds; however, excessive temperature or pressure can deform channels (41, 42). Following engraving, the PMMA layers were thermally bonded at 120 °C under 2 bar of pressure for 90 minutes to produce sealed microchannels. Raw semen samples were collected after 2–3 days of sexual abstinence and liquefied at 37 °C for 30 minutes. The samples were then introduced into the microchannels using a syringe pump at varying flow rates. Outlet fractions containing the separated sperm populations were collected into sterile tubes and immediately prepared for analysis. For each design, at least two independent semen samples were tested to evaluate reproducibility. Sperm quality assessment: Sperm concentration was determined using a hemocytometer. Motility, categorized as progressive, non-progressive, and immotile, was evaluated under a phase-contrast microscope.

Four ratchet-type microchannel geometries (Cases 1–4) were fabricated to evaluate the effects of channel dimensions and tooth structure on sperm separation efficiency. The geometrical parameters of each design are summarized in Table 1. The channel length represents the total length of the ratchet array from inlet to outlet; channel width denotes the lateral width of the flow passage; and channel height corresponds to the depth of the engraved microchannel. For ratchet structures, tooth base width is defined as the lateral dimension of the triangular tooth at its base, tooth spacing (pitch) is the center-to-center distance between consecutive teeth, and tooth angle is the acute angle formed between the tooth sidewall and the main channel axis. The measured geometrical parameters for all designs are listed below. These configurations were selected to cover a broad range of ratchet densities and angular deflections, enabling a comparative assessment of sperm hydrodynamic behavior and extraction efficiency.

Following fabrication of the microchannels and verification of their sealing integrity during fluid injection, fresh semen samples were obtained from the IVF laboratory of Afzalipour Hospital in Kerman. Each sample was loaded

into a syringe for delivery into the channels. A syringe pump, specifically designed and assembled by the research group at Shahid Bahonar University of Kerman, was employed to maintain constant injection rates of 0.017 and 0.034 mL/min. Using this system, semen was steadily introduced into the microchannels until a total volume of 1 mL had passed through, after which the collected effluent was retrieved from the outlet.

Table 1. Geometric dimensions of the ratchet microchannel designs

Case ID	Channel length (mm)	Channel width (mm)	Channel height (µm)	Tooth base width (mm)	Tooth spacing/pitch (mm)	Tooth angle (°)	Volume of extracted semen(ml)
Case 1	9.86	1.71	100 ± 5	-	200	-	0.1
Case 2	12.47	12.47	100 ± 5	variable	variable	variable	0.5
Case 3	53.55	15.37	100 ± 5	3.7	270	70	0.85
Case 4	36.34	15.22	100 ± 5	3.7	270	70	0.7

After approximately 30 or 60 minutes, corresponding to the injection of 1 mL of semen, the outlet port was closed, and the residual fluid was withdrawn back through the inlet. The recovered sperm were then prepared for microscopic evaluation. Experimental trials were performed for each of the four microchannel designs (Cases 1–4) using two to three independent semen samples obtained from patients diagnosed with low-quality semen. The number of replicates depended on sample availability and limitations in biological material. Each semen specimen was tested only once in a given geometry, resulting in two to three trials per channel design. After each experimental run, the effluent fractions (extracted outlet and vent outlet) were collected into sterile tubes, and the collected volumes were recorded to the nearest 10 µL using a calibrated pipette or by weighing. It should be noted that, due to capillary forces and sample surface tension, a small volume of semen inevitably remains as a residual film or trapped pocket in channel corners and microcavities following active collection. According to the study protocol, this residual fraction was not included in the "extracted" or "vent" fractions unless explicitly recovered by a controlled rinse step. To minimize artifacts and contamination risk, the following controls were adopted: (i) single-use devices—each microchannel was used for one sample and discarded to eliminate cross-sample carryover; (ii) aseptic handling and sterile collection—all efflux was collected into sterile, labeled tubes using sterile connectors and tips within the IVF laboratory; (iii) stable syringe-pump flow—the syringe pump provided a constant, uniform flow rate (Q) and steady pressure drop, which reduces trapping and local accumulation during operation; (iv) device cleaning and leak testing before use—channels were cleaned during fabrication (isopropanol rinse), thermally bonded, visually inspected, and leak-tested before each run; and (v) prompt downstream analysis—collected fractions were analyzed immediately (or stored briefly at a controlled temperature) to avoid post-collection biological changes.

It should be noted that the volume of semen extracted from the outlet channel after injection was not identical across all experiments. This variation arises from inherent differences in the surface tension and rheological properties of individual semen samples, which affect liquid drainage and residual film formation along the channel walls. Due to these factors, a small fraction of the injected sample remains trapped within microchannel corners and surface microcavities, preventing complete recovery. Consequently, the collected outlet volume represents an approximate value for each case rather than an absolute one. The average extracted volumes obtained for each microchannel configuration are presented in Table 1.

Sperm concentration, motility, and morphology were evaluated according to the World Health Organization (WHO, 2021) guidelines and strict Kruger criteria. Concentration, motility, and morphology were assessed under phase-contrast microscopy. To eliminate observer bias, all analyses were performed under fully blinded conditions. Processed and control samples were coded anonymously and placed in the standard analysis queue of the IVF Laboratory at Afzalipour Hospital (Kerman University of Medical Sciences). The coded samples were analyzed by an experienced and certified embryologist who was blinded to the sample identity, experimental group, and processing method. Decoding was performed only after completion of all measurements and data recording. This procedure ensured unbiased evaluation of sperm quality parameters across all experimental conditions.

Table 2. Estimated wall shear rate, wall shear stress, and Reynolds number for each microchannel geometry at the experimental flow rates

Case ID	Channel width (mm)	Channel height (µm)	Flow rate ($mL min^{-1}$)	Shear rate ($\times 10^3 s^{-1}$)	Shear stress (Pa)	Reynolds number
Case 1	1.71	100	0.017	5.96	5.96	5.8
Case 1	1.71	100	0.034	11.9	11.9	11.6
Case 2	12.47	100	0.017	0.82	0.82	20.1
Case 2	12.47	100	0.034	1.64	1.64	40.2
Case 3	15.37	100	0.017	1.10	1.10	37.3
Case 3	15.37	100	0.034	2.19	2.19	74.6
Case 4	15.22	100	0.017	1.11	1.11	37.0
Case 4	15.22	100	0.034	2.22	2.22	74.0

Hydraulic calculations and shear estimates

To quantify the mechanical environment experienced by sperm in the microchannels, order-of-magnitude estimates of wall shear rates, wall shear stresses, and hydraulic Reynolds numbers for the channel geometries reported in Table 1. For each geometry, the parallel-plate approximation was used $\gamma \dot{} w \approx 6Q/(w*h2)$ (valid for $h \ll w$) and $\tau w = \mu \gamma \dot{} w$ with $\mu = 1.0 \times 10\text{-}3$ Pa·s. Hydraulic diameter and Reynolds number were computed as $Dh = 2wh/(w+h)$ and $Re = \rho U avg Dh/\mu$ where $Uavg = Q/(w*h)$ and $\rho = 1000$ $kg \cdot m^{-3}$. Numerical results for representative operating conditions (Q = 0.017 and 0.034 $mL \cdot min^{-1}$) are presented in Table 2. These estimates are conservative, representing worst-case wall shear conditions, and were used to interpret the biological data reported in this study.

The shear and Reynolds number estimates show that the ratchet geometries used for motility-based selection operate in a laminar flow regime with sufficient residence time for active sperm navigation. However, they also produce relatively high wall shear rates (on the order of 10^3–10^4 s^{-1}, corresponding to shear stresses of about 1–20 Pa at our low-flow operating point). These values informed the selection of low Q for motility selection and the use of sperm DNA fragmentation (SDF) endpoints as a direct measure of biological impact.

The Sperm Retrieval Index

To quantify multi-dimensional changes in semen quality following microfluidic processing, SRI was used, a composite metric developed in this study that combines three clinically-relevant sperm parameters: total motility, normal morphology, and sperm concentration normalized to World Health Organization (WHO) (43) reference limits. The SRI provides a single quantitative score that reflects whether a processed sample reaches (or exceeds) minimum clinical quality thresholds and thus facilitates direct comparison among different microchannel designs and operating conditions.

(1):

$$SRI = \frac{(T_{out} * M_{out} * C_{out})}{(T_{WHO} * M_{WHO} * C_{WHO})} \qquad (1)$$

Where T_{out} is the total motility in the processed (output) sample, expressed as a percentage (%). Total motility is defined as the sum of progressive and non-progressive motility.

M_{out} is the percentage of sperm with normal morphology in the processed sample (%), assessed according to the morphology criteria described in the Methods section.

C_{out} is the sperm concentration in the processed sample (million $sperm \cdot mL^{-1}$).

T_{WHO}, M_{WHO}, C_{WHO} are the lower reference limits used for normalization (WHO reference values adopted for this study: total motility = 40%; normal morphology = 4%; concentration = 15 × 10^6 $sperm \cdot mL^{-1}$). An SRI value of 1 indicates that the processed sample, as a whole, matches the WHO lower reference limits on the three axes simultaneously. An SRI greater than 1 indicates that the processed sample exceeds these minimum thresholds; whereas an SRI less than 1 indicates that at least one normalized component remains below the WHO reference.

Results

The migration of motile sperm within confined microenvironments is strongly influenced by hydrodynamic interactions with surrounding boundaries. Numerous studies, including the seminal work by Denissenko et al. (2012), have shown that spermatozoa exhibit wall-following and rheotactic behaviors in response to local shear gradients, leading to preferential accumulation near surfaces and directed motion against the flow (30).

Table 3. Results from injecting two different sperm samples into the microchannel of Case 1 with a flow rate of 0.034 ml/min

Samples	Sample 1			Sample 2		
Location	input	extracted	vent	input	extracted	vent
Count (million/ml)	20	30	20	15	25	10
Progress%	40	60	30	15	30	5
Non-progress%	10	20	10	10	10	10
Immotile%	45	20	60	75	60	85
Morphology%	3	6	2	2	3	1
SRI	1.2500	6	0.67	0.47	2.5	0.062

These mechanisms are particularly relevant in microfluidic geometries, where controlled flow and surface topography can be leveraged to separate highly motile, morphologically normal sperm from the heterogeneous semen population. In the present study, these foundational insights are extended to experimentally quantify the influence of distinct ratchet-channel geometries on sperm migration patterns, motility enhancement, and overall retrieval efficiency under low–Reynolds-number flow conditions. According to the work of Denissenko et al. (2012), the ratchet geometry shown in Figure 1 was designed, manufactured, and tested (30). The results obtained from semen injection at a flow rate of 0.034 ml/min are reported in Table 3.

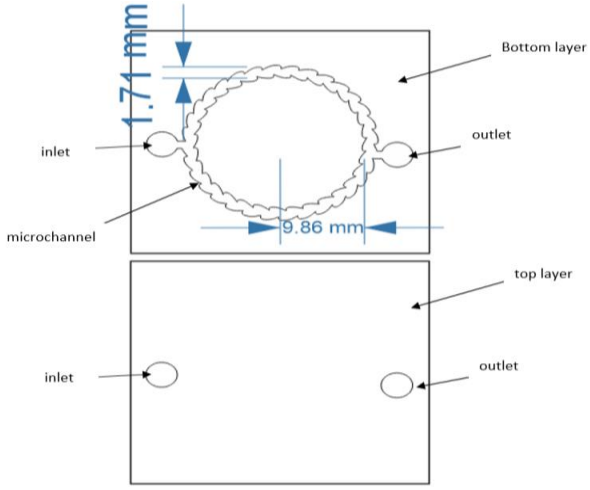

Figure 1. Schematic of a ratchet microchannel for separating motile sperm (case 1)

The terms used throughout all tables are defined as follows. Input refers to the raw, unprocessed semen sample injected into the device. Extracted denotes the concentrated output fraction collected from the retention zone, which is enriched with motile and morphologically normal sperm through ratchet trapping and rheotaxis. In contrast, the Vent represents the discarded effluent fraction, containing immotile sperm, debris, and seminal fluid that bypasses the ratchets.

Sperm motility was classified into three categories: Progressive Motility (Progress), defined as spermatozoa moving actively, either linearly or in a large circle, regardless of speed; Non-Progressive Motility (Non-progress), which includes all other patterns of active tail movement without forward progression, such as swimming in small circles; and Immotile, indicating a complete absence of active tail movement. Count (Sperm Concentration) was defined as the number of spermatozoa per milliliter of semen, expressed as 106 sperm per mL. Morphology represents the percentage of spermatozoa classified as morphologically normal, requiring the absence of abnormalities in the head, midpiece, principal piece (tail), and cytoplasmic residue.

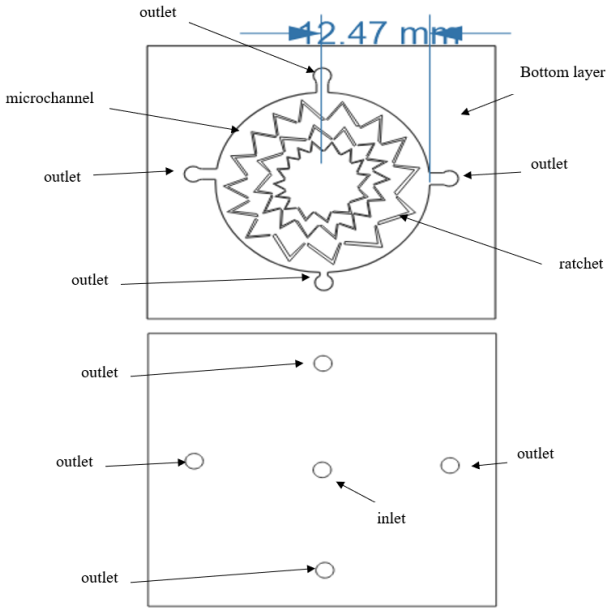

Figure 2. Schematic of a ratchet microchannel for separating motile sperm (case 2)

The results presented in Table 3 clearly show that the designed geometry has improved the quality of outgoing sperm; however, this improvement does not significantly enhance the channel's efficiency. Reducing the flow rate into the channel can decrease the velocity of the semen, which may cause a greater number of sperm to collide with

the walls of the channel, resulting in improved separation. In light of this, the previous experiment was conducted using two different sperm samples at a flow rate of 0.017 ml/min, and the results are presented in Table 4.

Table 4. Results from injecting two different sperm samples into the microchannel of Case 1 with a flow rate of 0.017 ml/min

Samples	Sample 1			Sample 2		
Location	input	extracted	vent	input	extracted	vent
Count (million/ml)	10	25	8	18	40	8
Progress%	20	35	10	15	40	10
Non-progress%	5	20	10	15	10	15
Immotile%	75	45	80	70	50	75
Morphology%	2	4	2	3	4	2
SRI	0.21	2.29	0.13	0.68	3.34	0.17

The results shown in Table 4 demonstrate an improvement compared to those in Table 3; however, they are still insufficient to justify the use of this geometry in assisted reproductive techniques. While further reducing the inlet flow rate may lead to better outcomes, the channel's efficiency for use in infertility laboratories is significantly compromised due to the excessive duration of the process. Therefore, a new ratchet geometry was designed to explore the potential for achieving better results than those obtained previously.

According to the research conducted by Guidobaldi et al. (2014), the geometry shown in Figure 2 was designed and fabricated with a specific function in mind (25). It was assumed that motile spermatozoa would become trapped in the rattling obstacles upon encountering them, which would facilitate their separation. In contrast, non-motile spermatozoa would be expelled along with the seminal fluid.

Two different semen fluids were injected into the channel at a flow rate of 0.034 ml/min, and the results obtained are presented in Table 5. These results indicate that the new geometry had less of an effect on sperm separation than the previous one.

It is evident from the results in Table 5 that this geometry and flow rate did not perform effectively in sperm separation, so channel case 2 was tested at a flow rate of 0.017 ml/min. The findings from this experiment are presented in Table 6.

The results clearly show that reducing the flow rate positively impacts sperm separation and improves quality; however, the improvements have not yet reached a significant level. Since further reductions in flow rate are unlikely to provide considerable benefits for the reasons mentioned earlier, an alternative geometry was designed to explore the possibility of achieving better sperm separation. The schematic of this geometry is shown in Figure 3.

The results of semen injection at a flow rate of 0.034 ml/min are shown in Table 7. This geometry successfully achieved a higher percentage of sperm recovery and separation compared to previous designs.

A flow rate of 0.017 mL/min was tested to explore the potential for achieving better separation in channel case 3. The results are shown in Table 8. Since these findings indicated a significant improvement in sperm recovery, the experiment was repeated with three different samples to verify accuracy and repeatability.

Due to the success of this geometry in enhancing sperm quality and separation, a design similar to Case 3 was developed (Figure 4) to explore the potential for further improvement. The main assumption underlying this design was that dividing the channel into two sections and rearranging the fluid flow, along with reducing the velocity of semen passage through the canal, could result in improved separation.

Table 5. Results from injecting two different sperm samples into the microchannel of Case 2 with a flow rate of 0.034 ml/min

Samples	Sample 1			Sample 2		
Location	input	extracted	vent	input	extracted	vent
Count (million/ml)	15	25	10	18	30	10
Progress%	38	35	20	30	40	5
Non-progress%	17	15	10	15	10	10
Immotile%	45	50	70	55	50	85
Morphology%	2	4	2	1	4	2
SRI	0.46	2.1	0.25	0.75	2.5	0.12

Table 6. Results from injecting two different sperm samples into the microchannel of Case 2 with a flow rate of 0.017 ml/min

Samples	Sample 1			Sample 2		
Location	input	extracted	vent	input	extracted	vent
Count (million/ml)	10	25	5	12	35	14
Progress%	18	30	8	10	20	22
Non-progress%	20	22	10	20	15	22
Immotile%	62	38	82	72	65	56
Morphology%	3	4	1	3	5	3
SRI	0.47	2.2	0.07	0.45	2.55	0.55

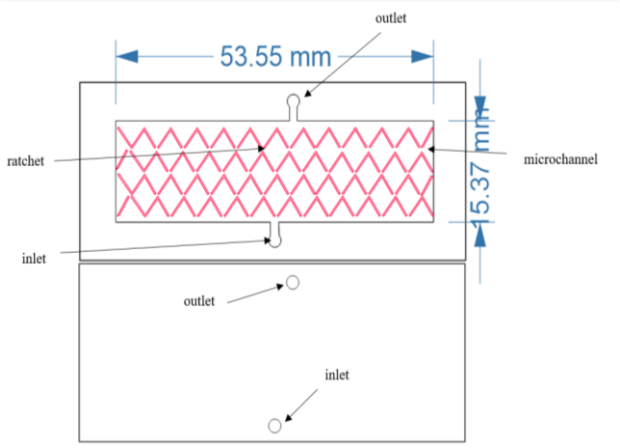

Figure 3. Schematic of a ratchet microchannel for separating motile sperm (case 3)

The results of semen injection at a flow rate of 0.017 are presented in Table 9. It is evident that this type of geometry performed better than the geometries used in Cases 1 and 2; however, the results were not significantly different from those of Case 3. Considering the larger size and higher manufacturing cost of this case compared to Case 3, it is advisable to select Case 3 as the suitable channel for this study.

Impact of ratchet microchannel design on SRI enhancement

To better assess how each microchannel configuration influenced sperm quality, the percentage improvement in SRI was determined by comparing the extracted fraction with its corresponding input, according to Equation ((2):

$$SRI\ increase = \frac{(SRI)_{\text{extracted}} - (SRI)_{input}}{(SRI)_{input}} \qquad (1)$$

This parameter integrates changes in motility, morphology, and concentration into a single value, allowing direct comparison of separation efficiency across all tested ratchet-based designs. When multiple semen samples were evaluated for a given geometry, the degree of improvement varied depending on the initial quality of the sample. To illustrate the maximum potential of each design, we report the result corresponding to the sample that achieved the greatest relative increase in SRI, which reflects the best performance achievable under favorable conditions. The comparison results are illustrated in the diagram presented in Figure 5.

The analysis of SRI values across different microchannel geometries reveals that channel design has a direct impact on sperm quality. For Case 1, the concentrated fraction showed a clear improvement in SRI compared to the input and vent fractions, confirming that the funnel-type ratchet geometry facilitates the retention of progressively motile sperm. However, the magnitude of improvement was moderate, and further optimization of the flow rate was required to achieve higher separation efficiency.

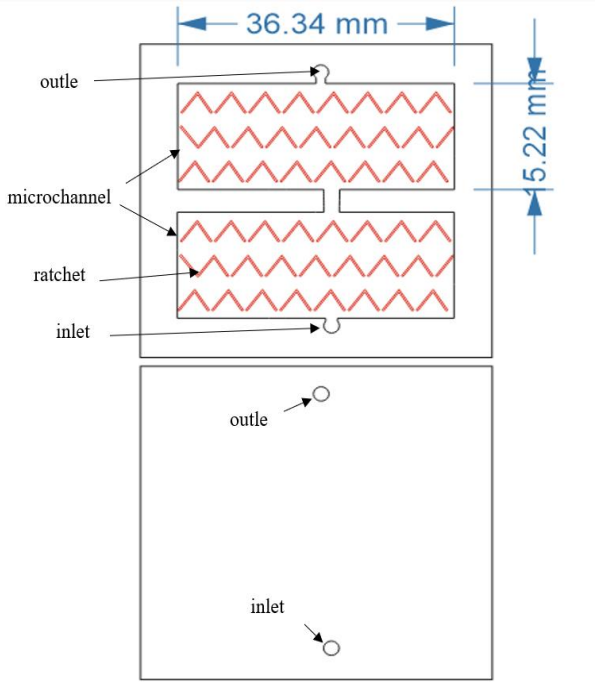

Figure 4: Schematic of a ratchet microchannel for separating motile sperm (case 4)

Table 7. Results from injecting two different sperm samples into the microchannel of Case 3 with a flow rate of 0.034 ml/min

Samples	Sample 1			Sample 2		
Location	input	extracted	vent	input	extracted	vent
Count (million/ml)	8	22	15	5	14	1-2
Progress%	20	35	6	20	25	2
Non-progress%	15	10	4	5	10	8
Immotile%	65	55	90	75	65	90
Morphology%	1	3	1	1	3	1
SRI	0.14	1.24	0.062	0.05	0.61	0.006

In Case 2, which incorporated trapping obstacles inspired by earlier studies, the outcomes demonstrated only partial improvement. While some enhancement in the concentrated fraction was observed, the efficiency was inconsistent and highly dependent on the input sample characteristics. This suggests that the obstacle arrangement did not adequately prevent low-quality sperm from remaining in the output stream.

A more substantial effect was noted in Case 3, where modifications to the channel geometry led to a greater degree of motile sperm enrichment. Reducing the flow rate in this configuration resulted in pronounced SRI gains for the concentrated samples, highlighting the role of controlled hydrodynamic interactions and wall-guided swimming in improving sperm selection. Importantly, this design consistently yielded higher recovery rates across multiple tested samples, suggesting greater robustness compared to earlier geometries.

Finally, Case 4 employed a two-stage arrangement intended to prolong sperm–wall interactions and promote additional filtration. Although the SRI values indicated some improvement over Cases 1 and 2, performance was comparable to that of Case 3. Considering that the latter design achieved similar outcomes with a simpler and more cost-effective structure, Case 3 appears to offer the most practical balance between device efficiency and manufacturability.

Overall, these findings emphasize that subtle modifications in channel geometry, combined with optimized flow rates, can markedly affect sperm recovery efficiency. The ratchet-inspired structures enhance sperm–boundary interactions, thereby enriching the concentrated fraction with higher-quality spermatozoa.

Table 8. Results from injecting two different sperm samples into the microchannel of Case 3 with a flow rate of 0.017 ml/min

Samples	Sample 1			Sample 2			Sample 3		
Location	input	extracted	vent	input	extracted	vent	input	extracted	vent
Count (million/ml)	2	9	1	9	40	11	2	8	2
Progress%	15	18	10	10	20	4	15	20	5
Non-progress%	5	3	0	6	10	10	7	5	5
Immotile%	80	79	90	84	70	86	78	75	90
Morphology%	1	4	1	1	3	1	1	4	1
SRI	0.016	0.31	0.0042	0.067	1.5	0.058	0.018	0.34	0.008

Table 9. Results from injecting two different sperm samples into the microchannel of Case 4 with a flow rate of 0.017 ml/min

Samples	Sample 1			Sample 2		
Location	input	extracted	vent	input	extracted	vent
Count (million/ml)	6	18	4	3	8	1
Progress%	15	20	0	10	18	10
Non-progress%	10	10	10	3	1	0
Immotile%	75	8	90	77	81	90
Morphology%	1	4	1	1	4	2
SRI	0.062	0.9	0.012	0.0163	0.25	0.008

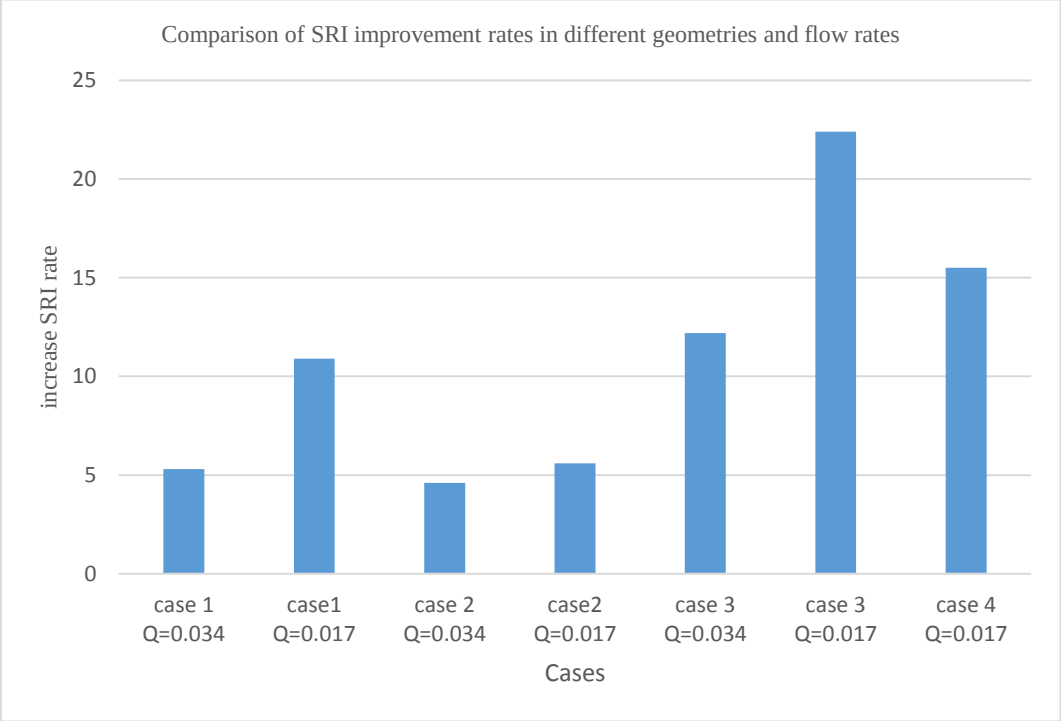

Figure 5. Chart comparing the improvement rates of SRI across various geometries and flow rates to enhance sperm sample quality

Discussion

This study demonstrates the effectiveness of ratchet-based microfluidic channels fabricated from PMMA via laser engraving in improving sperm separation and enhancing the quality of low-quality sperm samples. Across four systematically optimized channel designs, tested at two flow rates (0.034 mL/min and 0.017 mL/min), we achieved an average 2.5-fold increase in sperm concentration, with the best-performing configurations yielding up to a 4-fold increase in concentration (e.g., from 10 million/mL to 40 million/mL in Case 2, sample 2 at 0.017 mL/min) and more than a 20-fold improvement in the SRI, which integrates motility, morphology, and concentration relative to WHO standards. This passive, geometry-driven mechanism exploits sperm rheotactic behavior, boundary-following tendencies, and reorientation limitations to selectively guide and trap motile sperm while venting immotile cells, debris, and seminal fluid. The enriched, concentrated fraction was highly suitable for ART procedures such as ICSI. Variations across designs and flow rates were attributable to initial sperm quality, channel geometry (e.g., ratchet asymmetry, length, and density), and hydrodynamic conditions, which influenced trapping efficiency through sperm propulsion and wall interactions. No adverse effects on sperm viability were observed, and the lower flow rate (0.017 mL/min) consistently outperformed the higher rate by reducing shear stress and allowing more time for sperm accumulation. Each of the four designs provided insights into the interplay between geometry and fluid dynamics in sperm sorting. In all experiments, raw semen samples were injected using a syringe pump, with output fractions analyzed for reproducibility.

Case 1 (standard ratchet design with baseline asymmetry) demonstrated a 3-fold average increase in concentration and up to an approximately 11-fold improvement in SRI at the lower flow rate. The ratchets leveraged sperm's difficulty in reorienting against asymmetric barriers, as observed in bacterial and sperm models (24, 25), enabling the accumulation of progressively motile sperm while expelling non-motile ones through the vent. At 0.034 mL/min, gains were modest (e.g., an approximately 5-fold SRI in sample 1), reflecting higher shear that limited boundary-following time. Reducing the flow to 0.017 mL/min enhanced performance by prolonging residence time and allowing more effective hydrodynamic entrapment (3, 4, 6, 26). This case establishes a baseline, showing that even simple ratchet geometries can significantly enrich low-quality samples without centrifugation-induced ROS damage (3).

Case 2 (modified with increased ratchet density) tested the impact of additional barriers on separation efficiency. Performance improved slightly over Case 1 at lower flow rates, with approximately 4.5-fold SRI gains, indicating that denser ratchets create more collision opportunities for motile sperm to align and accumulate (28). However, at higher flow rates, results were comparable to Case 1, suggesting saturation, where excess barriers increase local

resistance and disrupt laminar flow, potentially allowing some motile sperm to bypass the ratchets (21). This finding aligns with studies showing that obstacle geometry modulates upstream swimming (25), emphasizing that density enhancements are most beneficial under gentle flows that mimic the female reproductive tract (44).

Case 3 (extended ratchet length and curvature) proved highly effective for severe low-quality samples, delivering up to a 4-fold concentration increase and 20-fold improvement in SRI at 0.017 mL/min (e.g., sample 2: 0.05 to 1.00). The longer, curved ratchets minimized reorientation time and maximized unidirectional transport, consistent with bacterial ratchet systems (26), trapping more than 90% immotile sperm in the vent while enriching motile fractions. Higher flow reduced efficiency (~8-fold SRI), likely due to increased drag that impeded boundary accumulation (30). With three samples tested at low flow, reproducibility was confirmed, highlighting curvature's role in reducing trapping inefficiencies compared to straight designs (45). This case was particularly advantageous for oligozoospermic samples, where initial counts were below 10 million/mL, by providing extended interaction paths without compromising morphology.

Case 4 (optimized hybrid design with angled constrictions, tested only at 0.017 mL/min) achieved approximately 3-fold concentration gains and up to 15-fold SRI improvements, building on prior cases by integrating features such as denser rows and curvature. The design balanced flow resistance with trapping sites, selectively retaining progressive sperm (up to 25%) while venting immotile debris (>90%). This outcome reflects enhanced rheotaxis and surface guidance (39, 44), making the design suitable for clinical integration. Compared to Case 3, the gains were similar, but higher in absolute SRI for some samples, suggesting hybrid geometries stabilize performance across variable inputs. The comparative performance of the four ratchet designs is consistent with a simple physical balance between selection opportunity (time and distance available for motile sperm to self-select) and geometric trapping (the frequency of stagnation or recirculation sites created by tooth density and sharp corners). Case 2, which implements a very dense ratchet array, produced more frequent corner encounters and local recirculation regions. These features increase the likelihood of non-selective trapping in which immotile and morphologically abnormal sperm become lodged in microcavities, increase collision frequency, and shorten the effective free path available for directional migration, all of which reduce the fraction of high-quality sperm recovered. By contrast, Case 3 combines a substantially longer channel length (providing longer residence time), a wider passage, and a larger tooth pitch with an acute tooth angle (70°); this geometry promotes wall-guided reorientation and rectified downstream motion of progressively motile sperm while minimizing stagnation zones and passive entrapment. The modest curvature in the extended channel additionally generates lateral shear gradients that bias motile swimmers toward the extraction outlet while leaving passive/defective sperm in the vented stream. Together, these geometric effects explain why Case 3 achieved the highest SRI and the most favorable motility and morphology outcomes: it provides sufficient selection time and favorable wall-interaction geometry without creating excessive trapping sites.

Together, these results emphasize that lower flow rates (0.017 mL/min) enhance enrichment by reducing shear and promoting natural sperm behaviors, while geometric variations such as channel length and ratchet density introduce trade-offs. Excessive complexity risks saturation and dilution, whereas optimal asymmetry (e.g., Cases 3 and 4) maximizes selectivity. These findings align with clinical and experimental studies reporting that microfluidics approaches improve sperm quality relative to conventional methods, which often induce DNA fragmentation (10, 17, 18, 46). Reported enhancements include motility (30–60%), morphology (2–4-fold), and reduced DNA damage (20–50%), leading to better ART outcomes (17). For instance, Heidarnejad et al. (2024) achieved higher motility with rheotaxis devices but lower concentration gains (~2-fold) than our maximum (4-fold) (17). Similarly, Asghar et al. (2014) and Chinnasamy et al. (2018) reported 2–5-fold morphology improvements with columnar arrays, consistent with the study mean (~3-fold) but below our peak in severe samples (19, 20). Huang et al. (2014) integrated laminar flow to achieve more than 90% viability, paralleling our stress-minimizing approach, although their throughput-focused design prioritized speed over enrichment (21). Ratchet-specific studies like Hulme et al. (2008) and Guidobaldi et al. (2014) demonstrated length-based sorting in bacteria and sperm, with 20–30% efficiency gains from curved geometries mirroring Case 3's superiority (24, 25). Karimi et al. (2025) showed conical barriers promoting alignment, analogous to this study's angled ratchets, while Denissenko et al. (2012) confirmed boundary-following in human sperm, underpinning mechanisms (28, 30).

Reviews by Huang et al. (2023) and Bouloorchi et al. (2024) report typical 2–4-fold concentration increases, aligning with the average observed, but are exceeded by optimized designs under low flow (29, 31). For context, non-microfluidic approaches such as density gradient methods yield approximately 2-fold gains, but with ROS risks (3), while swim-up offers gentle selection but low

yields (6, 8, 47). The presented system uniquely combines high fold improvements in low-quality samples with simple fabrication, offering advantages in resource-limited settings.

Strengths of this work include substantial SRI enhancements (>20-fold maximum), systematic evaluation of flow and geometry, and ethical use of discarded samples. Limitations include small sample sizes per case, focus on motility and morphology without direct DNA assays, and potential scalability issues for higher volumes. Future work should: (1) refine geometries for hybrid flow rates; (2) integrate with TUNEL or SCSA for DNA integrity; and (3) conduct clinical trials assessing fertilization and pregnancy rates. Ultimately, these ratchet designs could enhance ART by providing enriched, high-quality sperm from low-quality samples, complementing existing microfluidic platforms.

Conclusion

This work demonstrates that sperm recovery efficiency in microfluidic devices is highly dependent on channel geometry and operating conditions. By systematically comparing four ratchet-inspired designs, the study showed that concentrated outlet fractions consistently exhibited higher SRI values than the corresponding inputs, confirming the capability of microchannels to selectively enrich motile and morphologically normal sperm. The improvement was most pronounced in Case 3, which demonstrated greater reproducibility, efficiency, and reduced fabrication complexity compared with Case 1. Although reducing the inlet flow rate further enhanced separation efficiency, practical considerations such as increased processing time must be accounted for in clinical translation. Taken together, these results indicate that carefully engineered microfluidic ratchet structures can offer an efficient and non-invasive alternative to centrifugation-based sperm preparation. In particular, the Case 3 geometry provides a compelling balance of performance and simplicity, making it well suited for further clinical validation. Future studies involving larger patient cohorts and direct evaluation of DNA integrity and oxidative stress will be essential to confirm the translational potential of these devices. If successful, such systems may represent an important step toward safer, faster, and more reliable sperm selection in assisted reproduction.

Acknowledgements

The authors extend their heartfelt thanks to the director and staff of the IVF Department at Afzalipour Hospital in Kerman for their invaluable support and assistance. Their expertise and cooperation were essential to the successful completion of this research

Authors' Contributions

Saeed Derakhshan: conducted the research, performed data analysis, carried out experiments, and drafted and revised the manuscript. **Ataallah Kamyabi**: served as the supervisor, contributed to data analysis, and was responsible for revising and correcting the manuscript as well as being the corresponding author. **Sareh Ashourzadeh**: provided supervision, contributed to data analysis, and participated in the revision and review of the manuscript. **Tooraj Reza Mirshekari:** contributed to data analysis and assisted in the revision and correction of the manuscript.

Data Availability

The datasets and materials used and analyzed during the current study are available from the corresponding author upon reasonable request.

Ethical Approval

All procedures performed in this study were approved by the Research Ethics Committees of Shahid Bahonar University of Kerman (Ethics Code: ID: IR.UK.REC.1401.009). Written informed consent was obtained from all participants.

Conflict of Interest

The authors declare that they have no known competing financial interests or personal relationships that could have appeared to influence the work reported in this paper.

Consent for Publication

Not applicable.

Funding

This study did not receive any specific grant from funding agencies in the public, commercial, or not-for-profit sectors.

References

1. Marzano G, Chiriacò MS, Primiceri E, Dell'Aquila ME, Ramalho-Santos J, Zara V, et al. Sperm selection in assisted reproduction: a review of established

methods and cutting-edge possibilities. Biotechnology advances. 2020;40:107498. https://doi:10.1016/j.biotechadv.2019.107498
2. Eisenberg ML, Esteves SC, Lamb DJ, Hotaling JM, Giwercman A, Hwang K, et al. Male infertility. Nature Reviews Disease Primers. 2023;9(1):49. https://doi:10.1038/s41572-023-00459-w
3. Baldini D, Ferri D, Baldini GM, Lot D, Catino A, Vizziello D, et al. Sperm selection for ICSI: do we have a winner? Cells. 2021;10(12):3566. https://doi:10.3390/cells10123566
4. Dai C, Zhang Z, Shan G, Chu LT, Huang Z, Moskovtsev S, et al. Advances in sperm analysis: techniques, discoveries and applications. Nature Reviews Urology. 2021;18(8):447-467. https://doi:10.1038/s41585-021-00472-2
5. Leisinger CA, Vanderwall DK, Glazar BS, Sauber-Schatz EK, Remillard RL, Macpherson ML. Effect of microfluidic sperm separation vs. standard sperm washing processes on laboratory outcomes and clinical pregnancy rates in an unselected patient population. Reproductive Medicine. 2021;2(3):125-130. https://doi.org/10.3390/reprodmed2030013
6. Sheibak N, Amjadi FS, Raigani M, Aflatoonian R, Ramezani M, Maghsoudi R. Microfluidic sperm sorting selects a subpopulation of high-quality sperm with a higher potential for fertilization. Human Reproduction. 2024;39(5):902-911.https://doi.org/10.1093/humrep/deae045
7. Henkel RR, Schill WB. Sperm preparation for ART. Reproductive biology and endocrinology. 2003;1:108. https://doi:10.1186/1477-7827-1-108
8. Raad G, Bakos A, Loid M, Talarczyk-Desole J, Sugihara A, Pacey A, et al. Differential impact of four sperm preparation techniques on sperm motility, morphology, DNA fragmentation, acrosome status, oxidative stress, and mitochondrial activity: a prospective study. Andrology. 2021;9(5):1549-1559. https://doi:10.1111/andr.13038
9. Zhang F, Dai C, Zhang R, Sun Y. Application and progress of Raman spectroscopy in male reproductive system. Frontiers in Cell and Developmental Biology. 2022;9:823546. https://doi:10.3389/fcell.2021.823546
10. Agarwal A, Mulgund A, Hamada A, Chyatte MR. A unique view on male infertility around the globe. Reproductive biology and endocrinology. 2015;13:37. https://doi:10.1186/s12958-015-0032-1
11. Ribas-Maynou J, Yeste M, Salas-Huetos A. Clinical implications of sperm DNA damage in IVF and ICSI: updated systematic review and meta-analysis. Biological Reviews. 2021;96(4):1284-1300. https://doi:10.1111/brv.12700
12. Whitesides GM. The origins and the future of microfluidics. Nature. 2006;442(7101):368-373. https://doi:10.1038/nature05058
13. Seo Db, Agca Y, Feng Z, Critser JK. Development of sorting, aligning, and orienting motile sperm using microfluidic device operated by hydrostatic pressure. Microfluidics and Nanofluidics. 2007;3:561-570. https://doi:10.1007/s10404-006-0142-3
14. Cho BS, Schuster TG, Zhu X, Chang D, Smith GD, Takayama S. Passively driven integrated microfluidic system for separation of motile sperm. Analytical chemistry. 2003;75(7):1671-1675. https://doi:10.1021/ac020579e
15. Koyama S, Amarie D, Soini HA, Novotny MV, Jacobson SC. Chemotaxis assays of mouse sperm on microfluidic devices. Analytical chemistry. 2006;78(10):3354-3359. https://doi:10.1021/ac052087i
16. Smith GD, Swain JE, Bormann CL. Microfluidics for gametes, embryos, and embryonic stem cells. Seminars in reproductive medicine. 2011;29(1):5-14. https://doi:10.1055/s-0030-1268699
17. Heidarnejad A, Sadeghi M, Arasteh S, Ghiass MA. A novel microfluidic device for human sperm separation based on rheotaxis. Zygote. 2024:1-9. https://doi:10.1017/S0967199424000467
18. Phiphattanaphiphop C, Luesiri K, Kaewnoonual N, Thanomsuksinchai N, Phanphak S, Dangrat K, et al. A novel microfluidic chip-based sperm-sorting device constructed using design of experiment method. Scientific reports. 2020;10(1):17143. https://doi:10.1038/s41598-020-73841-3
19. Asghar W, Velasco V, Kingsley JL, Shoukat MS, Shafiee H, Anchan RM, et al. Selection of functional human sperm with higher DNA integrity and fewer reactive oxygen species. Advanced healthcare materials. 2014;3(10):1671-1679. https://doi:10.1002/adhm.201400058
20. Chinnasamy T, Kingsley JL, Inci F, Tandogan N, Allen JW, Carr MM, et al. Guidance and self-sorting of active swimmers: 3D periodic arrays increase persistence length of human sperm selecting for the fittest. Advanced Science. 2018;5(2):1700531. https://doi:10.1002/advs.201700531
21. Huang HY, Fu HT, Tseng HY, Huang CT, Lai CC, Yao DJ. Motile human sperm sorting by an integrated microfluidic system. Journal of Nanomedicine and Nanotechnology. 2014;5(3):1000199. https://doi:10.4172/2157-7439.1000199

22. Wu JK, Chen PC, Lin YN, Yu CW, Lin CM, Liu HL, et al. High-throughput flowing upstream sperm sorting in a retarding flow field for human semen analysis. Analyst. 2017;142(6):938-944. https://doi:10.1039/c6an02420c
23. Reichhardt CO, Reichhardt C. Ratchet effects in active matter systems. Annual Review of Condensed Matter Physics. 2017;8(1):51-75. https://doi:10.1146/annurev-conmatphys-031016-025522
24. Hulme SE, Shevkoplyas SS, Apfeld J, Fontana W, Whitesides GM. Using ratchets and sorters to fractionate motile cells of Escherichia coli by length. Lab on a Chip. 2008;8(11):1888-1895. https://doi:10.1039/b809892a
25. Guidobaldi A, Jeyaram Y, Berdakin I, Moshchalkov VV, Condat CA, Marconi V, et al. Geometrical guidance and trapping transition of human sperm cells. Physical Review E. 2014;89(3):032720. https://doi:10.1103/PhysRevE.89.032720
26. Coppola S, Kantsler V. Curved ratchets improve bacteria rectification in microfluidic devices. Physical Review E. 2021;104(1):014602. https://doi:10.1103/PhysRevE.104.014602
27. Huang J, Chen H, Li N, Zhao Y. Emerging microfluidic technologies for sperm sorting. Engineered Regeneration. 2023;4(2):161-169. https://doi:10.1016/j.engreg.2023.02.001
28. Karimi A, Yaghoobi M, Abbaspourrad A. Geometry of obstructed pathway regulates upstream navigational pattern of sperm population. Lab on a Chip. 2025;25(4):631-643. https://doi:10.1039/d4lc00797b
29. Bouloorchi Tabalvandani M, Saeidpour Z, Habibi Z, Zare M, Badieirostami M. Microfluidics as an emerging paradigm for assisted reproductive technology: a sperm separation perspective. Biomedical Microdevices. 2024;26(2):23. https://doi:10.1007/s10544-024-00705-2
30. Denissenko P, Kantsler V, Smith DJ, Kirkman-Brown J. Human spermatozoa migration in microchannels reveals boundary-following navigation. Proceedings of the National Academy of Sciences. 2012;109(21):8007-8010. https://doi:10.1073/pnas.1202934109
31. Huang J, Chen H, Li N, Zhao Y. Emerging microfluidic technologies for sperm sorting. Engineered Regeneration. 2023;4(2):161-169. https://doi:10.1016/j.engreg.2023.02.001
32. Gaffney EA, Gadêlha H, Smith DJ, Blake JR, Kirkman-Brown JC. Mammalian sperm motility: observation and theory. Annual Review of Fluid Mechanics. 2011;43(1):501-528. https://doi:10.1146/annurev-fluid-121108-145442
33. Howard J. Mechanics of motor proteins. In: Flyvbjerg H, Jülicher F, Ormos P, David F, editors. Physics of bio-molecules and cells. Berlin: Springer; 2002. p. 69-94. https://doi:10.1007/3-540-45701-1_2
34. Lindemann CB, Lesich KA. Flagellar and ciliary beating: the proven and the possible. Journal of cell science. 2010;123(4):519-528. https://doi:10.1242/jcs.051326
35. Gibbons IR, Rowe AJ. Dynein: a protein with adenosine triphosphatase activity from cilia. Science. 1965;149(3682):424-426. https://doi:10.1126/science.149.3682.424
36. Saggiorato G, Alvarez L, Jikeli JF, Kaupp UB, Gompper G, Elgeti J. Human sperm steer with second harmonics of the flagellar beat. Nature communications. 2017;8(1):1415. https://doi:10.1038/s41467-017-01462-y
37. Kaupp UB, Kashikar ND, Weyand I. Mechanisms of sperm chemotaxis. Annual Review of Physiology. 2008;70:93-117. https://doi:10.1146/annurev.physiol.70.113006.100654
38. Kantsler V, Dunkel J, Blayney M, Goldstein RE. Rheotaxis facilitates upstream navigation of mammalian sperm cells. eLife. 2014;3:e02403. https://doi:10.7554/eLife.02403
39. Woolley D, Vernon G. A study of helical and planar waves on sea urchin sperm flagella, with a theory of how they are generated. Journal of Experimental Biology. 2001;204(7):1333-1345. https://doi:10.1242/jeb.204.7.1333
40. Elgeti J, Gompper G. Microswimmers near surfaces. The European Physical Journal Special Topics. 2016;225:2333-2352. https://doi:10.1140/epjst/e2016-60070-6
41. Gabriel EFM, Coltro WKT, Garcia CD. Fast and versatile fabrication of PMMA microchip electrophoretic devices by laser engraving. Electrophoresis. 2014;35(16):2325-2332. https://doi:10.1002/elps.201300511
42. Tweedie M, Maguire P. Microfluidic ratio metering devices fabricated in PMMA by CO2 laser. Microsystem Technologies. 2021;27(1):47-58. https://doi:10.1007/s00542-020-04902-w
43. World Health Organization. WHO laboratory manual for the examination and processing of human semen. 6th ed. Geneva: World Health Organization; 2021.
44. Kantsler V, Dunkel J, Polin M, Goldstein RE. Ciliary contact interactions dominate surface scattering of

swimming eukaryotes. Proceedings of the National Academy of Sciences. 2013;110(4):1187-1192. https://doi:10.1073/pnas.1210548110

45. Reichhardt CO, Reichhardt C. Ratchet effects in active matter systems. Annual Review of Condensed Matter Physics. 2017;8:51-75. https://doi:10.1146/annurev-conmatphys-031016-025522
46. Ribas-Maynou J, Llavanera M, Mateo-Otero Y, Bonet S, Yeste M, Barranco I. Advanced sperm selection strategies as a treatment for infertile couples: a systematic review. International Journal of Molecular Sciences. 2022;23(22):13859. https://doi:10.3390/ijms232213859
47. Henkel RR, Schill WB. Sperm preparation for ART. Reproductive biology and endocrinology. 2003;1(1):108. https://doi:10.1186/1477-7827-1-108